

## Influence of the substrate-electrode applied bias voltage on the properties of sputtered a-C:H thin films

This article has been downloaded from IOPscience. Please scroll down to see the full text article.

2001 J. Phys.: Condens. Matter 13 3011

(<http://iopscience.iop.org/0953-8984/13/13/314>)

View [the table of contents for this issue](#), or go to the [journal homepage](#) for more

Download details:

IP Address: 171.66.16.226

The article was downloaded on 16/05/2010 at 11:45

Please note that [terms and conditions apply](#).

# Influence of the substrate-electrode applied bias voltage on the properties of sputtered a-C:H thin films

**Gabriel Lazar**

Bacău University, Calea Mărășești 157, Bacău, Romania

Received 30 October 2000, in final form 25 January 2001

## Abstract

Highly tetrahedral, hydrogenated amorphous carbon (a-C:H) films have been deposited using rf sputtering of graphite by a magnetron sputter source in Ar/CH<sub>4</sub> atmosphere. The deposition rate, the density and the structural properties of the deposited films were studied as a function of applied bias voltage on substrate during deposition. Optical emission spectroscopy was used to diagnose and monitor the plasma discharge. The film structure was studied using IR absorption spectroscopy. For all the films, the percentage of sp<sup>3</sup> hydrogen bonding is higher than 80%. The atomic percentage of bonding hydrogen in the films is in the range 40–60% and increases when the applied bias voltage is increasing.

## 1. Introduction

Hydrogenated amorphous diamond-like carbon (a-C:H) films are becoming increasingly important in several research areas of both pure and applied physics. The interest in these materials is based on their exceptional physical and chemical properties: high hardness and wear resistivity, chemical inertness to both acids and alkalis lack of magnetic response and an optical band gap ranging from 0 to a few electron volts depending upon deposition conditions. Practical applications in the fabrication of several thin films structures, such as multilayered x-ray mirrors, overcoats on media for magnetic and optical recording systems, protective and antireflection coatings for optical devices working in the infrared, protective coating in microelectronics etc, depend on the ability to produce films with suitable optical, electrical and mechanical properties [1–3]. The hydrogen concentration (up to 50%), giving the ratio of carbon single bondings (sp<sup>3</sup> coordination) to carbon double bondings (sp<sup>2</sup> coordination), depends on deposition parameters and governs all the properties [4]. Hydrogen stabilizes the dangling bonds of sp<sup>3</sup> carbon and increases the electrical resistivity and the optical gap. The higher the sp<sup>3</sup>/sp<sup>2</sup> ratio, the higher the electrical resistivity [4].

a-C:H has been prepared by plasma deposition from hydrocarbon gases [5–7], sputtering [4, 8], cathodic arc [9, 10], ion beam methods [11] and laser vaporization [12]. Common to all these methods is the deposition of a-C from particles whose energy is within the range of about 100 eV up to several kilo-electron volts [7]. Carbon films prepared by much lower energy methods such as evaporation have been reported to be electrically conducting [13]. It appears that the most critical process parameter determining the film properties is the ion

bombardment occurring during deposition [14]. Different models for describing the interaction of energetic ions with the amorphous network, such as preferential sputtering or displacement and the subplantation model, have been suggested [15]. In addition to several other techniques, which are capable of providing the requisite high energy density during film, deposition from hydrocarbon gases in rf discharges has become the most widely used [16]. During growth, the layers are subjected to ion bombardment controlled by the potential drop between the plasma potential and the negative dc bias voltage ( $V_b$ ) at the film surface. With increasing bombarding energy the film transforms from a soft polymer-like ( $V_b < 100$  V), to a hard diamond-like ( $100$  V  $< V_b < 600$  V) and finally to a soft graphite-like ( $V_b > 600$  V) material [14, 17]. The structure and hydrogen content as well as the properties of a-C:H films prepared by the PECVD technique depend also on the applied dc bias voltage [18].

The ion bombardment at the surface and processes in the plasma bulk can be separately controlled in a circular magnetron sputtering system. The magnetic field confines the electrons and improves gas decomposition and the bias voltage applied to substrate provides a selective control of the ion energies. The advantage of the magnetron sputter source is that this technique is widely established in industry and allows the deposition onto large areas with relatively high deposition rates. The use of suitable unbalanced magnetic-field configuration places the substrate immersed in the plasma so that the growing films is bombarded by energetic Ar ions from the plasma [8].

Structural characterization of a-C and a-C:H films has usually been carried out by Raman spectroscopy. The  $sp^3$  carbon component in the films, however, cannot be detected directly in Raman spectroscopy owing to the resonance Raman effect of unsaturated carbon bonding component. Recently, the ratios of  $sp^2$  to  $sp^3$  carbon components in the films were estimated by infrared IR spectroscopy and electron energy loss spectroscopy [9].

In this work, I study the variation of the structural properties of the deposited films as a function of applied bias voltage in the region  $-400$  V  $< U_p < 400$  V.

## 2. Experiment

a-C:H films were deposited by magnetron sputtering technique, using a pure graphite target, 7.5 cm in radius and 99.99% pure Ar/CH<sub>4</sub> gas mixture. The use of the methane gas in the sputtering deposition of amorphous carbon lead to an increasing of the deposition rate and the  $sp^3$  carbon proportion [19, 20]. The magnetron installation shown in figure 1 was built in our laboratory in order to deposit thin films by dc and rf planar and circular magnetron sputtering [21–23]. In an unbalanced magnetron, the plasma extends over both the target and the substrate, so that the Ar ions provide both the sputtering flux to the graphite target and the ion plating flux on the growing film. The energy and the flux of the ions (mainly Ar<sup>+</sup> and CH<sub>n</sub><sup>+</sup>) reaching the growing film surface were varied by applying an external bias voltage (from  $-400$  V to  $+400$  V) to the substrate. The plasma must also decompose the methane gas, for a better hydrogenation of films. The contribution of CVD process in the film growth is the object of further studies. A high flux of neutral C atoms is achieved by placing the magnets as close as possible to the graphite target. The configuration of the magnetic field is a critical parameter controlling the deposition rate and the ion plating intensity [8] and is a particular property of the magnetron.

The sputtering system used in this work is shown in figure 1. The films were deposited by rf circular magnetron sputtering, using an rf source at 13.56 MHz coupled at electrode 8 (figure 1). A stabilized dc power supply with maximum ratings 500 V and 240 mA connected at electrode 7 (figure 1) was used for negative or positive substrate polarization. Films were deposited on glass and silicon (both p and n types, 8–12 Ω cm resistivity) substrates at a

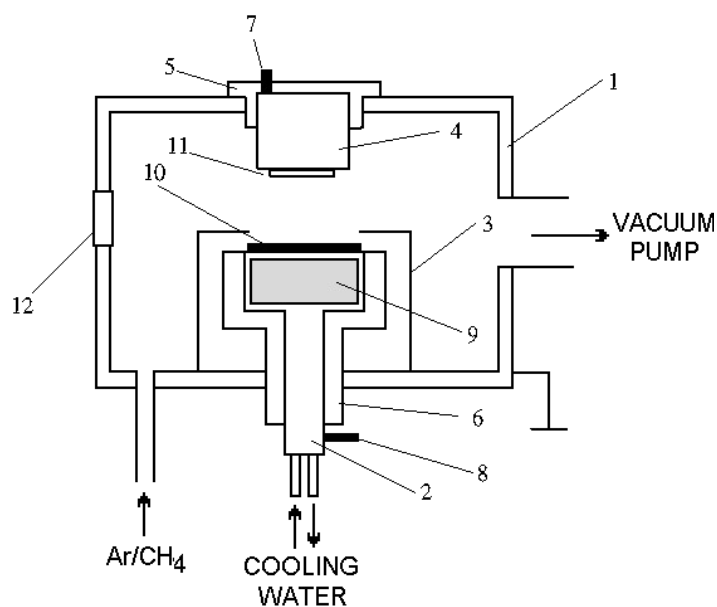


**Figure 1.** The sputtering system: 1—cylindrical stainless-steel chamber; 2—cathode; 3—circular anode; 4—planar anode; 5, 6—isolators; 7, 8—electrodes; 9—magnets; 10—target; 11—substrate; 12—window.

target-to-substrate distance of 3 cm. The volumetric proportion between Ar and methane was maintained constant at 1/1. The pressure during deposition was between 0.2 and 0.01 Torr. The substrate temperature remains below 100 °C for all samples. During deposition the substrates are partially masked so that thickness measurements can be made by Tolansky instruments. The densities of a-C:H coatings were determined by the quartz resonance method and by weighing substrates before and after thin film deposition and dividing the difference by the known film volume. The growth rate and film density were investigated against deposition pressure and applied dc bias voltage.

The reactive radicals in plasma were identified and analysed by optical emission spectrometry (OES). IR transmission of films deposited on Si substrates was measured with an IR SPECORD double beam spectrophotometer. Spectra were recorded in the wavenumber range from 1300 to 4600  $\text{cm}^{-1}$ . In the IR absorption spectra the most important information can be gained by inspecting the shape of the  $\text{CH}_x$  stretching absorption peak. First, we proceed to a deconvolution of the total absorption by C–H bonds into individual absorption peaks representing the specific stretching vibration frequency (3050  $\text{cm}^{-1}$  aromatic  $\text{sp}^2$  CH, 3020  $\text{cm}^{-1}$   $\text{sp}^2$   $\text{CH}_2$  olefinic, 3000  $\text{cm}^{-1}$  olefinic  $\text{sp}^2$  CH, 2960  $\text{cm}^{-1}$  antisymmetric  $\text{sp}^3$   $\text{CH}_3$ , 2950  $\text{cm}^{-1}$  olefinic  $\text{sp}^2$   $\text{CH}_2$ , 2925  $\text{cm}^{-1}$  antisymmetric  $\text{sp}^3$   $\text{CH}_2$ , 2915  $\text{cm}^{-1}$   $\text{sp}^3$  CH, 2870  $\text{cm}^{-1}$  symmetric  $\text{sp}^3$   $\text{CH}_3$ , 2855  $\text{cm}^{-1}$  symmetric  $\text{sp}^3$   $\text{CH}_2$ ) [24]. Each absorption peak is represented by a Gaussian function, which has been proven to give a good result [25]. The  $\text{sp}^3$  and  $\text{sp}^2$  intensities were simply calculated by integrating the various absorption peaks.

The hydrogen content was evaluated using the expression [14]

$$H_{tot} = A_s(\text{CH}_x) \int \frac{\alpha(k)}{k} dk$$

where  $\alpha(k)$  is the absorption coefficient at wavenumber  $k$ . The integration was performed over the absorption peak corresponding to the  $\text{CH}_x$  stretching vibrations around  $k = 3000 \text{ cm}^{-1}$ .

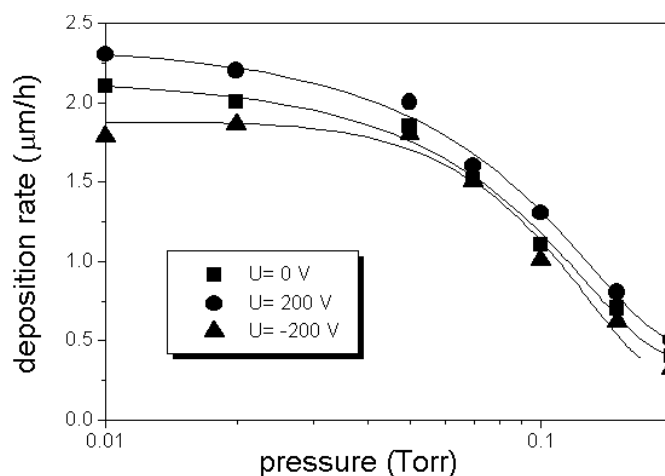


**Figure 2.** Dependence of deposition rate on the deposition gas pressure, for three different bias voltages, with 70 W rf power and 3–6 W dc power, glass substrate.

The absorption cross-section  $A_s(\text{CH}_x)$  is assumed to be equal to  $1.0 \times 10^{21} \text{ cm}^{-2}$  [14]. The atomic percentage of bonding hydrogen in the films is calculated based on determinate film density.

### 3. Results and discussion

Generally, with a bias voltage between  $-200 \text{ V}$  and  $+400 \text{ V}$  I obtained transparent and smooth films, colourless for pressures around 0.2 Torr and soft yellow when the deposition pressure is lowered to 0.01 Torr. For a bias voltage below  $-200 \text{ V}$  the bombardment of the argon ions on the substrate is very strong and the colour of deposited films is modified to a non-transparent dark brown. The high mechanical internal stress in carbon films reduces their adhesion on the substrate for films thickness over  $1 \mu\text{m}$ , but, below this value, the adhesion on glass and silicon is very good.

#### 3.1. Deposition rate

The deposition rate is an important parameter for method and installation evaluation. Figure 2 shows the dependence of deposition rate on the deposition gas pressure, for three different bias voltages. An rf power between 70 W for 0.01 Torr gas pressure and 40 W for 0.2 Torr gas pressure was used. The value of the discharge power was imposed by the gas pressure, for a constant rf signal generated by the source. The dc power for  $-200 \text{ V}$  bias voltage was 3 W and 6 W for  $+200 \text{ V}$  bias voltage. The deposition rate decrease with rising pressure and the shape of curve is given by the variation of discharge power. This variation of deposition rate with pressure is different from that found for a-C:H deposited from a glow discharge, where the growth rate increases when the gas pressure increase [26–29]. Figure 3 illustrates the increase of the deposition rate proportionally to the rf discharge power.

Figure 4 shows an increasing of growth rate with increasing bias voltage. The dc power increases from 0 to 40 W for positive biasing and from 0 to 8 W for negative biasing. I explain this increasing of the deposition rate by two effects: (a) for positive bias on the substrate, the combined rf–dc power of the discharge increases when bias voltage increases; (b) for negative bias

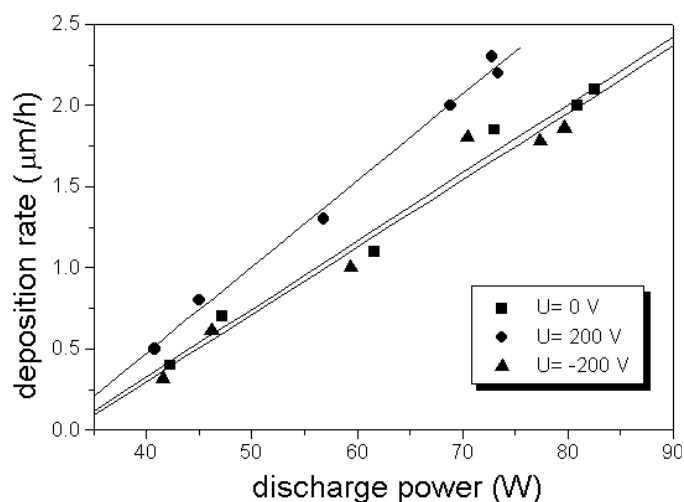


Figure 3. Deposition rate depending on discharge power.

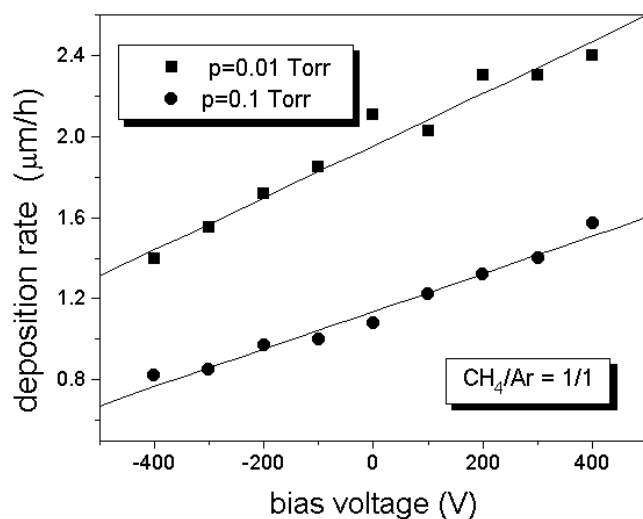
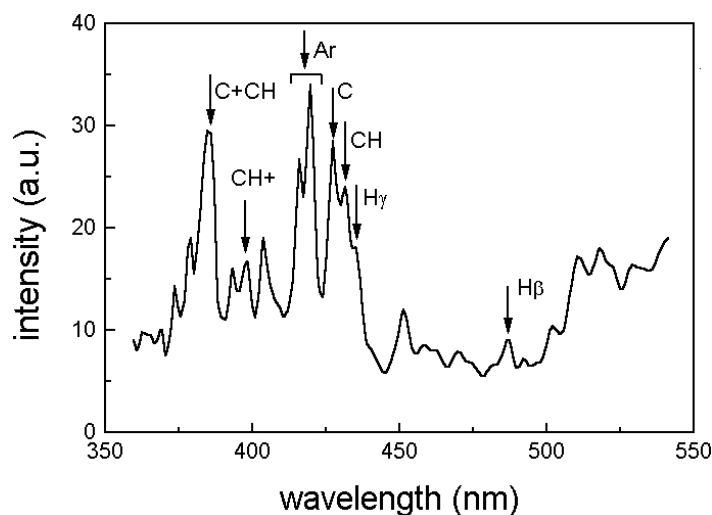


Figure 4. Deposition rate depending on bias voltage, with 70 W rf power, glass substrate.

on the substrate, the backsputtering yield increases according to Sigmund's theory [30] proportional to bias voltage. This is in contradiction with the results found for films prepared by rf plasma decomposition of hydrocarbon gases [27], but, in the rf plasma decomposition method, the negative bias on the substrate increases with the rf power. The rising of deposition rate in this case is determined not by the increase of negative bias but by the increasing of rf power.

The experimental results obtained for deposition rate using rf magnetron sputtering are similar to results obtained for pulsed laser deposition [31] or hot-filament chemical vapour deposition [32] and greater than usual values indicated for rf plasma decomposition,  $0.3\text{--}0.8\ \mu\text{m h}^{-1}$  [26–29]. In the work [33] deposition rates of  $2.5\ \mu\text{m h}^{-1}$  are reported for amorphous carbon deposited by dc magnetron sputtering, but with discharge power much greater, around 900 W.



**Figure 5.** Emission spectrum from discharge used for a-C:H film deposition at 15 mTorr, with 0 V bias voltage and 70 W rf power.

### 3.2. Optical emission spectroscopy

Optical emission spectroscopy (OES) was used to diagnose and monitor the plasma discharges generated in a  $\text{CH}_4 + \text{Ar}$  gas atmosphere, used for the a-C:H deposition. This technique has proven to be an effective tool in determining the gas intermediate species participating in the reaction mechanisms. In figure 5, a typical emission spectrum of the  $\text{CH}_4/\text{Ar}$  discharge is shown, corresponding to a deposition gas pressure of 15 mTorr, with 0 V bias voltage and 70 W rf discharge power. The most important features in the rf discharge are the Ar emission lines in the range 415–420 nm [16]. The spectrum basically presents the emission peaks corresponding to CH (390 nm and 431 nm),  $\text{H}_\beta$  (486 nm),  $\text{H}_\gamma$  (434 nm) and C (427 nm and 392 nm).

### 3.3. Density

The film density is necessary for calculation of the atomic percentage of bonding hydrogen in the films. Figure 6 illustrates the increase of the density with rising bias voltage, for both positive and negative polarization. The increase of positive or negative bias voltage cause an increase of the energy of the particles which bombard the film during growth and, accordingly, a greater densification of the material. For a positive applied bias, the system works like a combined circular rf–planar dc magnetron sputtering system, with a greater efficiency, reflected in a greater density. Also, this is the major reason for the decrease of the density when deposition pressure increases (figure 7). When the deposition pressure increases, the free path of deposition species decreases, leading to a decrease of the substrate bombardment and to a decrease of the density.

The density ranges between  $1.7$  and  $2.2 \text{ g cm}^{-3}$  and is lower than in crystalline carbon modifications (diamond:  $3.5 \text{ g cm}^{-3}$ , graphite:  $2.3 \text{ g cm}^{-3}$ ) but greater than usual values indicated for rf plasma decomposition ( $1.5\text{--}1.8 \text{ g cm}^{-3}$  [3, 7]) and in agreement with other results obtained for sputtered films [8].

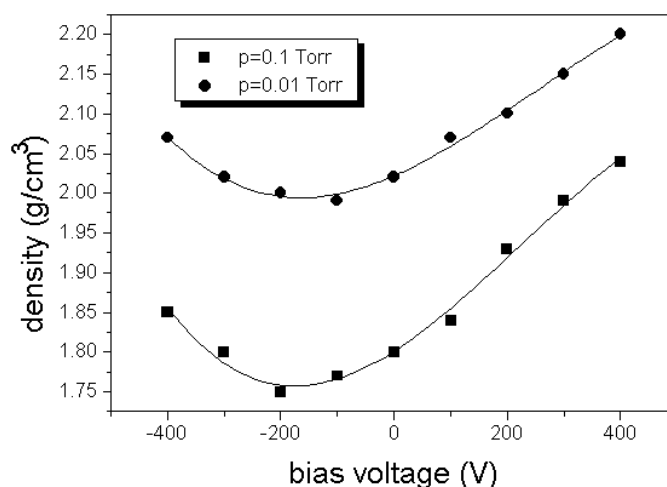


Figure 6. Density versus bias voltage.

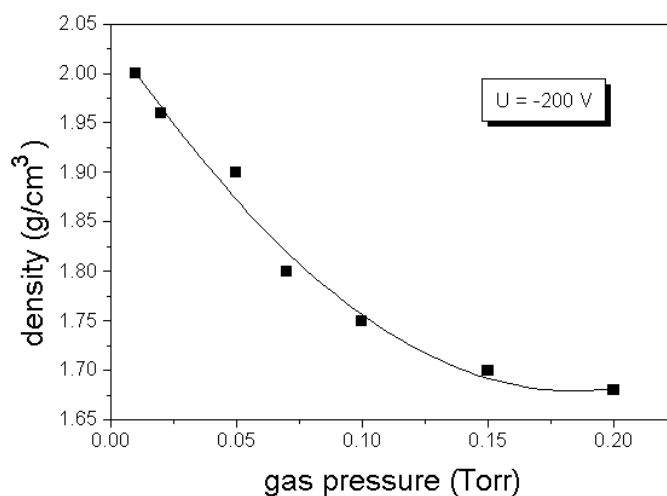


Figure 7. Density as a function of gas pressure.

### 3.4. Infrared absorption

In figure 8 a typical IR transmission spectrum of an a-C:H film is shown over a wide wave number range. The spectrum shows clear interference patterns. These are caused by multiple reflection in the deposited films and indicate a good optical quality of the material. In this spectrum absorption by carbon-hydrogen vibrations in the films is clearly visible around  $2950\text{ cm}^{-1}$ . The absorption band at  $2800\text{--}3000\text{ cm}^{-1}$  is associated with  $\text{sp}^3$  coordinated carbon [3, 4, 24, 25]. There are other infrared peaks observed for the amorphous carbon films. The deformation peaks of  $\text{sp}^3\text{ C-CH}_3$  are at  $1375$  and  $1450\text{ cm}^{-1}$  and a small peak due to  $\text{C=C}$  ( $\text{sp}^2$  bonding) at  $1600\text{ cm}^{-1}$  [34].

In figure 9 is presented the infrared absorption spectrum for the C-H stretching mode region for a sample obtained in following conditions: working gas  $\text{Ar/CH}_4 = 1/1$ , gas pressure  $10^{-2}$  Torr and substrate negative bias voltage 200 V. The properties of the film are:



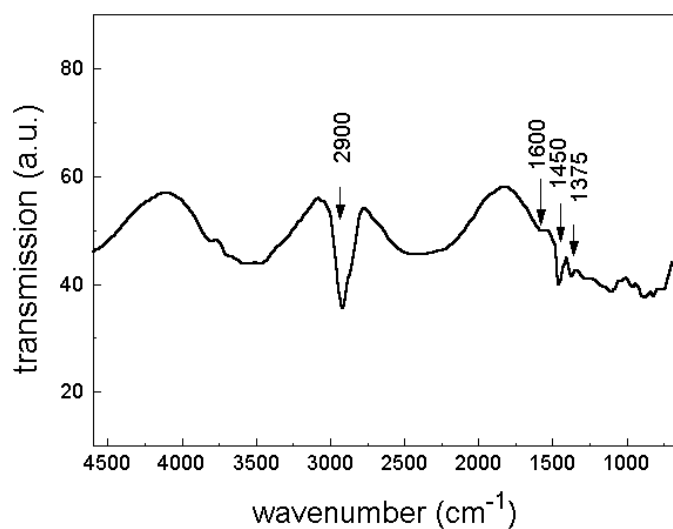


**Figure 8.** The IR transmission spectrum for a sample obtained in the following conditions: working gas Ar/CH<sub>4</sub> = 1/1, gas pressure 0.01 Torr, silicon substrate, 70 W rf power and substrate negative bias voltage 200 V.

thickness 1.8  $\mu\text{m}$ , refraction index 1.57 and optical band gap 2.17 eV. The spectrum can clearly be decomposed to seven Gaussian components, as shown in figure 9. The positions of these components are in very good agreement with other results [3, 14, 16, 24–26] and are summarized in table 1. It may be concluded from the great difference between  $\text{sp}^3$  and  $\text{sp}^2$  peak area that the type of bonding of C adjacent to H is predominantly  $\text{sp}^3$ . The small amplitude of 2960  $\text{cm}^{-1}$  and 2875  $\text{cm}^{-1}$  absorption maxima, which are ascribed to polymer-like material [14], indicates a diamond-like structure.

**Table 1.** C–H stretch absorption bands deconvoluted from the figure 9 absorption peak.

Curve number	Vibration frequency ( $\text{cm}^{-1}$ )		Configuration
	Observed	Predicted <sup>a</sup>	
1	3020.9	3020	$\text{sp}^2$ CH <sub>2</sub> (olefinic)
2	2999.6	3000	$\text{sp}^2$ CH (olefinic)
3	2960.0	2960–2970	$\text{sp}^3$ CH <sub>3</sub> (asymmetrical)
4	2924.1	2920–2925	$\text{sp}^3$ CH <sub>2</sub> (asymmetrical)
5	2914.6	2915–2920	$\text{sp}^3$ CH
6	2875.3	2865–2875	$\text{sp}^3$ CH <sub>3</sub> (symmetrical)
7	2854.3	2850–2855	$\text{sp}^3$ CH <sub>2</sub> (symmetrical)

<sup>a</sup> References [3], [14], [15], [23], [24] and [34].

### 3.5. Hydrogen content

Figure 10 shows the variation of bonding hydrogen atomic percentage and the  $\text{sp}^3$  proportion ( $\text{sp}^3 + \text{sp}^2 = 100\%$ ) in a-C:H films with applied bias voltages for two deposition gas pressures. The proportion of tetrahedral-bonded carbon has a low variation and indicates a high tetrahedral structure. The  $\text{sp}^3$  fraction is found to have its highest values for applied bias voltage in the

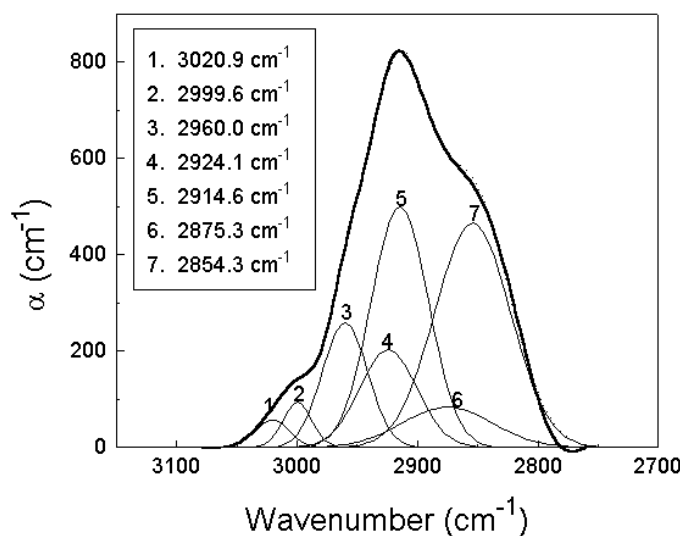


**Figure 9.** IR absorption peak of  $\text{CH}_x$  stretching vibrations centered at  $2900\text{cm}^{-1}$  with the curve fit for a sample obtained in the following conditions: working gas  $\text{Ar}/\text{CH}_4 = 1/1$ , gas pressure  $10^{-2}$  Torr and substrate negative bias voltage 200 V. The corresponding vibration frequencies are shown in the figure.

range  $-300\text{ V}$ – $200\text{ V}$ . The increase of bias voltage from  $-100\text{ V}$  to  $+400\text{ V}$  lead to a reduction of  $\text{sp}^3$  coordinated carbon proportion in the films. This result is qualitatively in line with the measurements of other publications [28] and indicates the influence of the ion bombardment at the layer surface. The hydrogen content, between 47 and 55% shows a high hydrogenation of the films. In contrast to other results, the increasing of hydrogen content is correlated with tetrahedral carbon proportion decreasing. I explain this relation by an increasing of cross-linking (more C–C bonding) with increasing argon bombardment of the films during growth (when negative bias voltage increases). In contrast, the increase of the energy of sputtered carbon leads to a higher hydrogenation of films.

#### 4. Conclusions

a-C:H films have been deposited by a combined rf circular magnetron sputtering and a CVD process in an  $\text{Ar}/\text{CH}_4$  gas mixture with additional external dc biasing of the substrate electrode. The variations of the structural properties of the deposited films as a function of applied bias voltage in the region  $-400\text{ V} < U_p < 400\text{ V}$  were investigated. The contribution of the CVD process in the film growth is the object of further studies.

Good values for deposition rate are obtained. When positive bias voltage increases, the growth rate increases due to increasing of discharge power. For negative bias on the substrate, the backsputtering yield increases proportional to bias voltage and the growth rate decreases.

The infrared absorption spectra and density results indicate a dominant diamond-like structure. The proportion of tetrahedral-bonded carbon and the hydrogen content were found to be correlated with the energy of incident species to the substrate. When the applied bias voltage increase from  $-200\text{ V}$  to  $+200\text{ V}$ , the density and  $\text{sp}^3$  fraction increase and hydrogen content decrease. I explain this by a favoured cross-linking (C–C bondings) when the energy of the sputtered carbon increase. Over 200 V bias voltage, the increase of the sputtered carbon

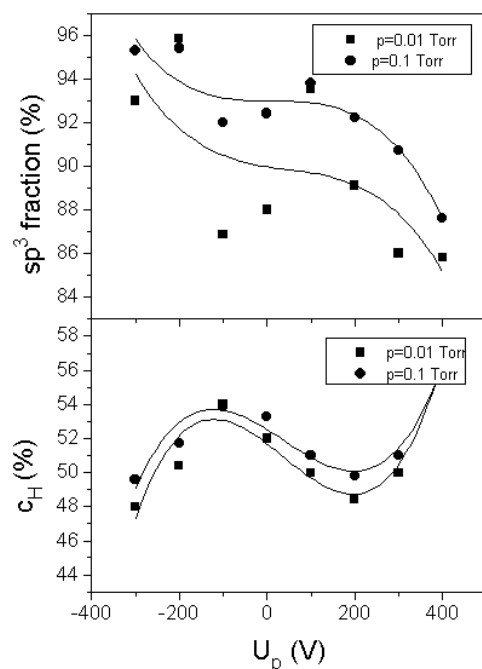


**Figure 10.** Atomic percentage of hydrogen and the  $sp^3$  proportion in a-C:H films as a function of the applied bias voltages for two deposition gas pressures.

energy leads to an increase of density, but the graphite sputtered species increase the  $sp^2$  carbon proportion. When the negative bias voltage increases, the positive ions accelerated by the negative bias decrease the incorporated hydrogen [35] and lead to the increase in the density.

### Acknowledgments

This work was supported by The Romanian National University Research Council (CNCSIS). The author is grateful to Mr I Vascan and to Mr M Caraman for expert technical assistance.

### References

- [1] Yañez-Limón J M, Ruiz F, González-Hernández J, Vázquez-López C and López-Cruz E 1994 *J. Appl. Phys.* **76** 3443
- [2] Lee J H, Lee Y H and Farouk B 1996 *J. Appl. Phys.* **79** 7676
- [3] Buuron A J M, van de Sanden M C M, van Ooij W J, Driessens R M A and Schram D C 1996 *J. Appl. Phys.* **78** 528
- [4] Pawlak F, Dufour Ch, Laurent A, Paumier E, Perriere J, Stoquert J P and Toulemonde M 1999 *Nucl. Instrum. Methods B* **151** 140
- [5] Gago R, Sanchez-Garrido O, Climent-Font A, Albella J M, Roman E, Raisanen J and Rauhala E 1999 *Thin Solid Films* **338** 88
- [6] Inoue Y, Komoguchi T, Nakata H and Takai O 1998 *Thin Solid Films* **322** 41
- [7] Bubenzer A, Dischler B, Brandt G and Koidl P 1983 *J. Appl. Phys.* **54** 4590
- [8] Schwan J, Ulrich S, Roth H, Ehrhardt H, Silva S R P, Robertson J, Samlenski R and Brenn R 1996 *J. Appl. Phys.* **79** 1416
- [9] Taki Y and Takai O 1998 *Thin Solid Films* **316** 45

- [10] Xu S, Cheah L K and Tay B K 1998 *Thin Solid Films* **312** 160
- [11] Brusa R S, Somoza A, Huck H, Tiengo N, Karwasz G P, Zecca A, Reinoso M and Halac E B 1999 *Appl. Sur. Sci.* **150** 202
- [12] Pappas D L, Saenger K L, Bruley J, Krakow W, Cuomo J J, Gu Tierer and Collins R W 1992 *J. Appl. Phys.* **71** 5675
- [13] Anderson D A 1977 *Phil. Mag.* **35** 17
- [14] Dekempeneer E H A, Jacobs R, Smeets J, Meneve J, Eersels L, Blanpain B, Roos J and Oostra D J 1992 *Thin Solid Films* **217** 56
- [15] Reinke P, Jacob W and Moller W 1993 *J. Appl. Phys.* **74** 1354
- [16] Martinu L, Raveh A, Dominique A, Bertrand L, Klemberg-Sapieha J E, Gujrathi S C and Wertheimer M R 1992 *Thin Solid Films* **208** 42
- [17] Jiang X, Zou J W, Reichelt C and Grunberg P 1989 *J. Appl. Phys.* **66** 56
- [18] Xu Niankan, Yin Dachuan, Liu Zhengtang and Zhengang Xiulin 1997 *J. Phys. D: Appl. Phys.* **30** 763
- [19] Mansano R D, Massi M, Zambom L S, Verdonck P, Nogueira P M, Maciel H S and Otani C 2000 *Thin Solid Films* **373** 243
- [20] Sanchez N A, Rincon C, Zambrano G, Galindo H and Prieto P 2000 *Thin Solid Films* **373** 247
- [21] Lazar I and Vascan I 1998 *Rom. J. Phys.* **43** 333
- [22] Lazar I and Vascan I 1997 *Balkan Phys. Lett.* **5** 693
- [23] Stamate M and Vascan I 1997 *Rom. J. Optoelectron.* **5** 47
- [24] Baba K, Aikawa Y and Shohata N 1991 *J. Appl. Phys.* **69** 7313
- [25] Gielen J W A M, Kleuskens P R M, van de Sanden M C M, Dekempeneer E H A and Meneve J 1996 *J. Appl. Phys.* **80** 5986
- [26] Mutsukura N, Inoue S and Machi Y 1992 *J. Appl. Phys.* **72** 43
- [27] Chou L H 1992 *J. Appl. Phys.* **72** 2027
- [28] Zou J W, Reichelt K, Schmidt K and Dischler B 1989 *J. Appl. Phys.* **65** 3914
- [29] Hoshino S, Fujii K, Shohata N, Yamaguchi H, Tsukamoto Y and Yanagisawa M 1989 *J. Appl. Phys.* **65** 1918
- [30] Sigmund P 1969 *Phys. Rev.* **184** 383
- [31] Li Z F, Yang Z Y and Xiao R F 1996 *J. Appl. Phys.* **80** 5398
- [32] Bohr S, Haubner R and Lux B 1996 *Appl. Phys. Lett.* **68** 1075
- [33] Richter F, Bewilogua K, Kupfer H, Muhling I, Rau B, Rother B and Schumacher D 1992 *Thin Solid Films* **212** 245
- [34] Seo Soon-Cheon, Ingram D C and Richardson H H 1995 *J. Vac. Sci. Technol. A* **13** 2856
- [35] Nakayama M, Tsuyoshi A, Shibahara M, Maruyama K and Kamata K 1995 *J. Vac. Sci. Technol. A* **13** 195